Computational Study of Turbulent Hydrogen Dispersion Hazards in a Closed Space

Rahul Angal*, Anupam Dewan** and K A Subramanian***

Commercial use of hydrogen in hydrogen-powered vehicles is still in experimentation, but in future, hydrogen will be used for vehicles as a fuel. The safety guidelines have to be provided when hydrogen is used commercially in vehicles. Using advanced computational fluid dynamics tools it is possible to investigate different properties during an accidental release of hydrogen, when it is used in an engine as a fuel. CFD tools also enable one to study different environmental conditions. In the present paper, the accidental release of hydrogen is modeled as the release of hydrogen from a small opening in a high pressure pipe line. The geometry considered is explored to find out the quantitative and qualitative mixing of hydrogen release. The simulations show the hydrogen distribution at different times. The present dispersion patterns give the idea of flammable zones and safety guidelines for the use of hydrogen in closed spaces. The paper also presents the capabilities of different RANS-based turbulence models to predict the patterns of hydrogen dispersion in closed spaces.

***Keywords*:** Hydrogen dispersion, Turbulence, CFD, Alternate fuels

Introduction

With intensified energy and environmental concerns, hydrogen is considered to be one of the most viable solutions to an ever increasing demand for clean energy. Although nowadays hydrogen is transported through the pressure vessels or produced directly at places where it is required, when hydrogen is used in large-scale, the transportation of hydrogen through pipelines would be the best option. The transformation from conventional fuel to such technology also requires public acceptance. However, unfortunately, risk is associated with this technology, because hydrogen disperses quickly unlike other gases, as it is one of the lightest gases and it

* M. Tech. Student, Department of Applied Mechanics, Indian Institute of Technology, Hauz Khas, New Delhi 110016, India. E-mail: rahulangal@gmail.com

** Professor, Department of Applied Mechanics, Indian Institute of Technology, Hauz Khas, New Delhi 110016, India; and is the corresponding author. E-mail: adewan@am.iitd.ac.in

*** Assistant Professor, Center for Energy Studies, Department of Applied Mechanics, Indian Institute of Technology, Hauz Khas, New Delhi 110016, India. E-mail: subra@ces.iitd.ernet.in

© 2012 IUP. All Rights Reserved.

has a very wide range of flammability limits (4% to 75% by volume). Therefore, it can be easily ignited even in a very lean mixture and this causes major risk with the use of hydrogen.

Wilkening and Baraldi (2007) compared natural gas pipeline with hydrogen leakage, as the behavior of natural gas pipeline is very well established and this technology is widely accepted. Similarly, Olvera and Choudhuri (2006) simulated hydrogen and methane dispersions around actual cubical buildings. They compared their results with the corresponding towing-tank data and other numerical results. They assessed the impact of release of methane and hydrogen around buildings under several environmental conditions such as no wind and when wind is blowing.

Gallego *et al*. (2007) and Vudumu and Koylu (2009) worked to establish the benchmark problem so that complex practical problems can be examined by validating the results with those of the benchmark problem. Vudumu and Koylu (2009) simulated different configurations such as a flow driven by buoyancy only, laminar flow and the condition if hydrogen is at the top of vessel. They considered different top conditions such as open top, closed top and partially closed top conditions. The open top condition is similar to the open environment gas release and this represents gas release from pipelines. The release of hydrogen in case of closed spaces, such as garages, etc., can be similar to the closed or partially closed top conditions. They developed a CFD model by taking into account the effect of buoyancy on the flow behavior and solved the energy, momentum and species transport equations. They examined the situation leading to a sudden release of hydrogen in air. They assumed the flow to be laminar only. Gallego *et al*. (2007) formulated benchmark problem based on the release of hydrogen mixing and dispersion in a closed vessel at subsonic speeds. Gallego *et al.* (2007) used different codes, grid sizes and different turbulence models to assess the effect of different factors on hydrogen dispersion. They chose a closed vessel problem due to its relevance in practical problems such as the release of hydrogen in closed spaces like garages, industries, etc.

Venetsanos *et al.* (2003) proposed a mathematical model for the actual Stockholm accident and investigated its safety point of view. The results predicted by Venetsanos *et al.* (2003) were in good agreement with the corresponding accidental results. The predicted results were similar in different regions of the flow field which include the near field damage, near wall damages and far field damages as well. They also conducted experiments on an actual accidental hydrogen release situation.

Olvera and Choudhuri (2006) simulated hydrogen and methane dispersion around actual cubical buildings. They compared their results with the towing-tank data and

other computational results reported in the literature. Their objective was to determine the optimal sensor location and to establish venting in the hydrogen fuel equipped buildings without using CFD. They assessed the impact of release of methane and hydrogen around buildings under several environmental conditions, such as when wind is blowing and when wind is not blowing. The dispersion pattern showed the risk associated with hydrogen in comparison with methane patterns. Their results illustrated the strong influence of the buoyant force on the dispersion pattern of hydrogen. Swain *et al.* (2003) performed experiments on helium. Since helium is the next lighter element after hydrogen, helium can be used for experimentation instead of hydrogen, as experimentation with hydrogen is both risky and expensive. Helium is an inert gas and therefore its usage is not risky, and it can be used in experiments involving leakage and dispersion; however, it cannot be replaced in experiments on combustion.

Major classification of gas leakage can be done as open, partially open and closed and the corresponding dispersion properties can be investigated in case of all three situations. For all three cases, the associated risks are different because different parameters are important in different situations. For example, in the case of closed space, the risk is more due to total volume of hydrogen compared to that due to volume flow rate of hydrogen, but in case of open environment, the flow rate is the dominant parameter for risk. This is because in a closed space, hydrogen gets accumulated and in open space, hydrogen flows out of the domain and therefore in a closed space risk is large if the volume of hydrogen released is large. But in case of open space, large flow rate results in large rate of mixing of hydrogen in regions close to the leakage. However, for partially closed space, both volume flow rate and volume of hydrogen are equally important, as in the case of partially closed domain (such as garages) hydrogen can accumulate and disperse due to the obstacle in its path. Therefore, large volume will result in large accumulation and the rate of dispersion will be directly proportional to the flow rate of hydrogen.

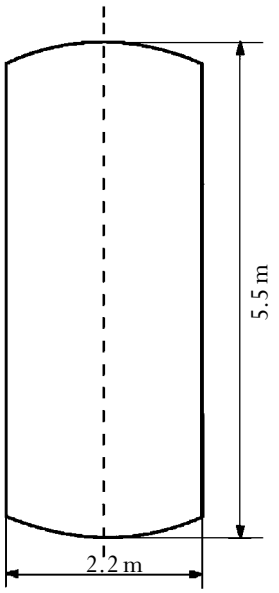
Complex dispersion patterns of hydrogen can be studied and compared with the help of the advanced CFD tools. Efficient use of different turbulence models is an added advantage with CFD. We can assess the performance of different turbulence models and accordingly select an appropriate model according to flow conditions and requirements of accuracy. For the present work, commercial, finite volume-based code FLUENT 6.3.26 is used to compute the hydrogen dispersion and the flammable zones of hydrogen when it is leaked into a closed space. In the situation of hydrogen leak in a confined space, it is important to find out hydrogen volume at different locations. One of the objectives of the present study is to find out the

turbulence model which closely predicts the dispersion patterns and the flammable zones as well. The present simulation can be considered as the benchmark problem for the turbulent hydrogen leak in closed spaces.

2. Geometry

The same geometry, as that considered by Shebeko *et al.* (1988) for their experimental investigation, is considered in the present study. The present computations are also compared with the experimental data of Shebeko *et al.* (1988), who considered a practical situation involving release of hydrogen in confined or closed spaces, e.g., garages, tunnels, etc. In such situations, hydrogen is released through very small openings and high pressure at sonic speeds. The vessel geometry considered by Shebeko *et al.* (1988) is shown in Figure 1. The vessel has a height of 5.5 m and diameter of 2.2 m. The closed vessel is initially filled up by the quiescent air at atmospheric pressure (101,325 Pa) and temperature (20 ^{0}C). Hydrogen is released vertically upward at a flow rate of 4.5l per s for 60 s. The injection tube diameter is 10.0 mm and the corresponding hydrogen release velocity is 58.0 m/s. They used six thermocatalytic sensors located at vertical axis of the cylindrical vessel at various positions to measure the volume fraction of hydrogen. They reported a precision of the measurement $\pm$0.2%. The sensors were located at $l_1 = 0.14$, $l_2 = 1.00$, $l_3 = 2.00$, $l_4 = 2.83$, $l_5 = 3.91$, $l_6 = 5.27$ m from the cylinder top.

Figure 1: Geometry Considered for the Present Computation



3. Mathematical Model and Boundary Conditions

The turbulent flow field was obtained by numerically solving the governing Reynolds-Averaged Navier-Stokes (RANS) equations using the finite volume method. Four different RANS-based turbulence models, namely, standard k-ε, RNG k-ε and realizable k-ε and k-ω, were used to model the effect of turbulence. The flow was also simulated by assuming the axisymmetric flow. Based on the grid independence study, a total of 81,330 elements were used for the computations (Figure 2). An unstructured mesh was used for the simulations which consisted of a fine grid in the vicinity of the axis to accurately capture hydrogen injection. The detailed meshed geometry as well as boundary conditions are shown in Figure 3. All the walls in the computational domain were treated as the solid wall because a closed container is considered in the present study. Based on the experimental conditions used by Shebeko *et al.* (1988), the hydrogen inlet velocity of 58.0 m/s was considered in the present study. Similarly, hydrogen was released at constant flow rate for initial 60 s.

The set of transient equations for conservation of mass, momentum, energy as well as non-reacting transport equations (for two species hydrogen and air) were solved numerically. These equations can be written in the tensor form as:

Figure 2: Hydrogen Volume Fraction After 0.5 s

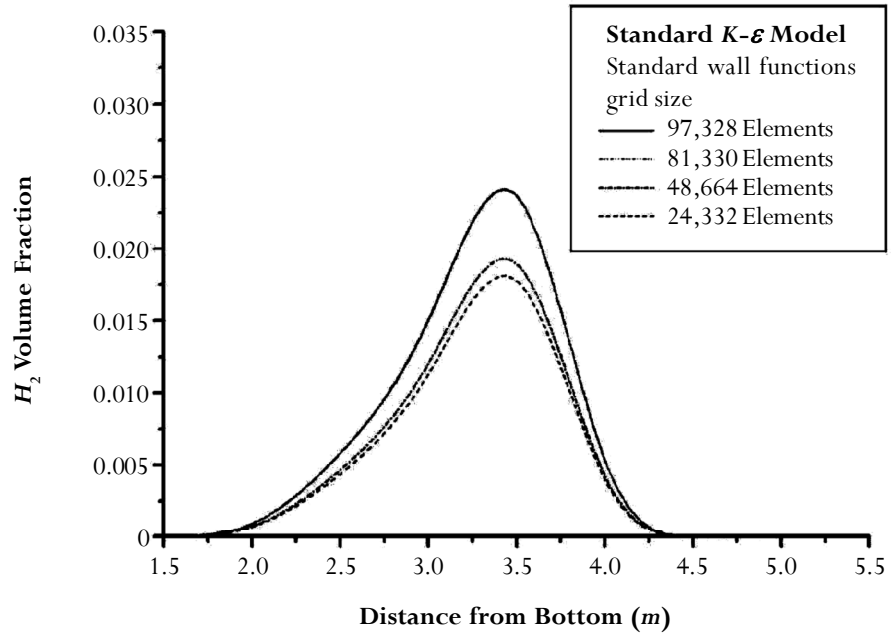
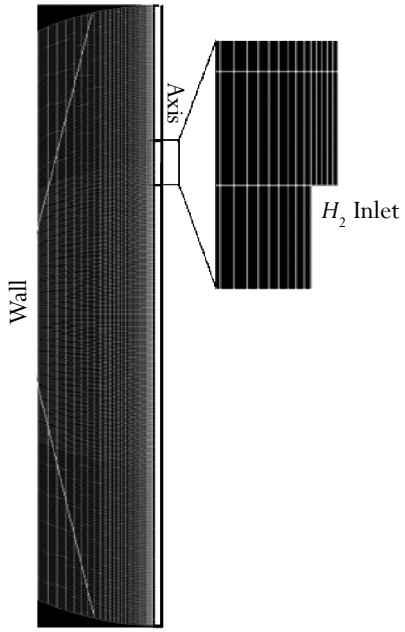


Figure 3: Detailed Meshed Geometry



Mass Conservation Equation

$$\frac{\partial \rho}{\partial t} + \frac{\partial}{\partial x_j}(\rho U_j) = 0 \qquad \ldots(1)$$

Momentum Equation

$$\frac{\partial U_i}{\partial t} + \frac{\partial}{\partial x_j}(\rho U_i U_j) = -\frac{\partial P}{\partial x_i} + \frac{\partial}{\partial x_j}\left[\mu\left(\frac{\partial U_i}{\partial x_j} + \frac{\partial U_j}{\partial x_i}\right) - \rho\overline{u_i' u_j'}\right] \qquad \ldots(2)$$

Energy Conservation Equation

$$\frac{\partial}{\partial t}(\rho E) + \frac{\partial}{\partial x_j}[U_i(\rho E + p)] = \frac{\partial}{\partial x_j}\left[(k + \frac{c_p \mu_t}{\mathrm{Pr}_t})\frac{\partial T}{\partial x_j} + U_i(\tau_{ij})_{eff}\right] \qquad \ldots(3)$$

where

$$(\tau_{ij})_{eff} = \mu_{eff}\left(\frac{\partial U_j}{\partial x_i} + \frac{\partial U_i}{\partial x_j}\right) - \frac{2}{3}\mu_{eff}\frac{\partial U_k}{\partial x_k}\delta_{ij} \qquad \ldots(4)$$

Species Transport Equation

The conservation equation to predict mass fractions for the i^{th} species, Y_i is given by:

$$\frac{\partial}{\partial t}(\rho Y_j) + \frac{\partial}{\partial x_j}(\rho U_j Y_j) = -\frac{\partial}{\partial x_j}(J_j) + R_j + S_j \quad \ldots(5)$$

where R_i denotes the net rate of production of species i by the chemical reaction and S_i the source term.

Mass Diffusion

For Laminar Flow: $J_j = -\rho D_j \nabla Y_j$ …(6)

For Turbulent Flow: $J_j = -(\rho D_j + \frac{\mu_t}{Sc_t})\nabla Y_j$ …(7)

For turbulent calculations, four RANS-based turbulence models, namely, standard k-ε, realizable k-ε, RNG k-ε and k-ω were used.

3.1 Standard k-ε model

In the k-ε model, k and ε are used to define velocity and scales. The basic assumption is that the production and the destruction terms of the dissipation equation vary with corresponding terms of the k-equation (Versteeg and Malalasekera, 2007). The standard k-ε model is the simplest model for which only boundary conditions need to be defined. It is known to perform well for most industrial flows and it is a well-established model as well. All two equation models are computationally expensive compared to the mixing length models (Dewan, 2011). The k-ε model fails to accurately capture flow behavior of some confined flows, large strained flows or rotating flows. The corresponding governing equations (Launder and Spalding, 1974) may be written as:

Turbulence kinetic energy (k):

$$\frac{\partial}{\partial t}(\rho k) + \frac{\partial}{\partial x_i}(\rho k u_i) = \frac{\partial}{\partial x_j}\left[\left(\mu + \frac{\mu_t}{\sigma_k}\right)\frac{\partial k}{\partial x_j}\right] + G_k + G_b - \rho\varepsilon + S_k \quad \ldots(8)$$

Dissipation rate (ε):

$$\frac{\partial}{\partial t}(\rho \varepsilon) + \frac{\partial}{\partial x_i}(\rho \varepsilon u_i) = \frac{\partial}{\partial x_j}\left[\left(\mu + \frac{\mu_t}{\sigma_k}\right)\frac{\partial \varepsilon}{\partial x_j}\right] + C_{1\varepsilon}\frac{\varepsilon}{k}(G_k + C_{3\varepsilon}G_b) - C_{2\varepsilon}\rho\frac{\varepsilon^2}{k} + S_\varepsilon \quad \ldots(9)$$

3.2 RNG k-ε Model

The RNG procedure removes small-scale motion from the governing equation by expressing their effects in terms of larger-scale motions and modified viscosity. The RNG k-ε model performs better than the standard k-ε model in case of expanding duct and similar flows (FLUENT Inc., 2006). The corresponding transport equations (Choudhury, 1993) may be written as:

Turbulence kinetic energy (k):

$$\frac{\partial}{\partial t}(\rho k)+\frac{\partial}{\partial x_i}(\rho k u_i)=\frac{\partial}{\partial x_j}\left[\alpha_k \mu_{eff}\frac{\partial k}{\partial x_j}\right]+G_k+G_b-\rho\varepsilon+S_k \qquad \ldots(10)$$

Dissipation rate (ε):

$$\frac{\partial}{\partial t}(\rho \varepsilon)+\frac{\partial}{\partial x_i}(\rho \varepsilon u_i)=\frac{\partial}{\partial x_j}\left[\alpha_k \mu_{eff}\frac{\partial \varepsilon}{\partial x_j}\right]+C_{1\varepsilon}\frac{\varepsilon}{k}(G_k+C_{3\varepsilon}G_b)-C_{2\varepsilon}\rho\frac{\varepsilon^2}{k}-R_\varepsilon+S_\varepsilon \qquad \ldots(11)$$

3.3 Realizable k-ε Model

This model has different formulation for turbulent viscosity. Further, a new transport equation for the dissipation rate ε is obtained from an exact equation for the transport of the mean-square vorticity fluctuations. The realizable k-ε model works well for plane and round jets. But it produces nonphysical turbulent viscosities in situations when the computational domain contains both rotating and stationary fluid zones (Shih *et al.*, 1995). The corresponding equations may be written as:

Turbulence kinetic energy (k):

$$\frac{\partial}{\partial t}(\rho k)+\frac{\partial}{\partial x_i}(\rho k u_i)=\frac{\partial}{\partial x_j}\left[\left(\mu+\frac{\mu_1}{\sigma_k}\right)\frac{\partial k}{\partial x_j}\right]+G_k+G_b-\rho\varepsilon+S_k \qquad \ldots(12)$$

Dissipation rate (ε):

$$\frac{\partial}{\partial t}(\rho \varepsilon)+\frac{\partial}{\partial x_j}(\rho \varepsilon u_j)=\frac{\partial}{\partial x_j}\left[\left(\mu+\frac{\mu_t}{\sigma_\varepsilon}\right)\frac{\partial \varepsilon}{\partial x_j}\right]+\rho C_1 S_\varepsilon-\rho C_2\frac{\varepsilon^2}{k+\sqrt{v\varepsilon}}+\left(C_{1\varepsilon}\frac{\varepsilon}{k}+C_{3\varepsilon}G_b\right)+S_\varepsilon \qquad \ldots(13)$$

where $C_1 = \max\left[0.43, \frac{\eta}{\eta+5}\right], \eta = S\frac{k}{\varepsilon}, S = \sqrt{2S_{ij}S_{ij}}$

In Equations (8) to (13), G_k denotes the generation of turbulence kinetic energy due to mean velocity gradient and G_b the generation of turbulence kinetic energy due to buoyancy. Here S_k and S_ε denote the source terms in the model, respectively. σ_k and σ_ε denote the turbulent Prandtl numbers for k and ε, respectively.

3.4 Standard k-ω Model

The k-ω model is based on the modeled transport equations for the turbulence kinetic energy (k) and the specific dissipation rate (ω), which can also be written as the ratio of ε to k. The model works well with low-Reynolds-number and is also applicable to wall-bounded flows, as these modifications are incorporated in equations itself. The turbulence kinetic energy and specific dissipation rate are obtained from the following transport equations (Wilcox, 1998).

Turbulence kinetic energy (k):

$$\frac{\partial}{\partial t}(\rho k) + \frac{\partial}{\partial x_i}(\rho k u_i) = \frac{\partial}{\partial x_j}\left(\Gamma_k \frac{\partial k}{\partial x_j}\right) + G_k - Y_k + S_k \quad \ldots(14)$$

Specific dissipation rate (ω):

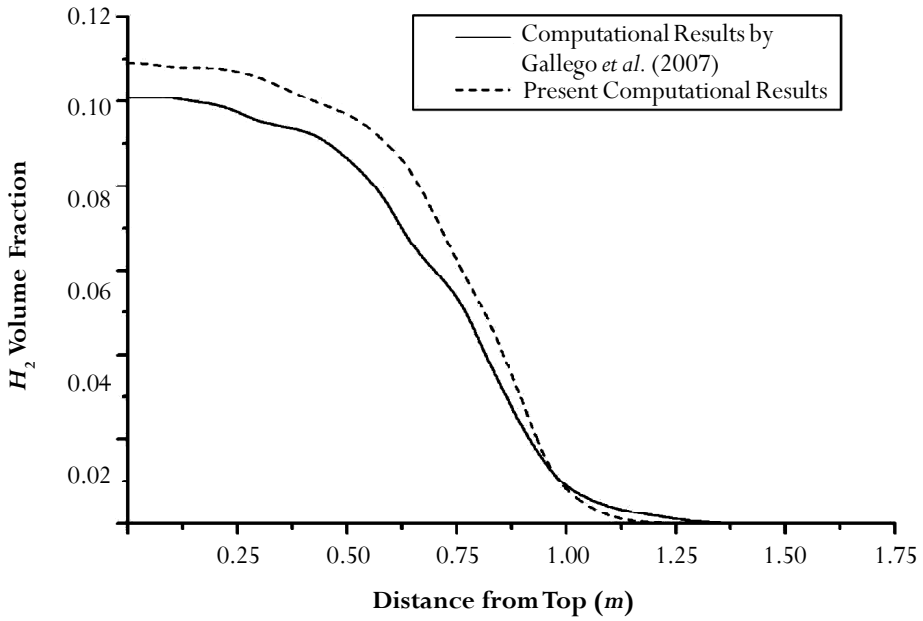
$$\frac{\partial}{\partial t}(\rho \omega) + \frac{\partial}{\partial x_i}(\rho \omega u_i) = \frac{\partial}{\partial x_j}\left(\Gamma_\omega \frac{\partial \omega}{\partial x_j}\right) + G_\omega - Y_\omega + S_\omega \quad \ldots(15)$$

4. Methodology and Code Validation

Flow field was obtained by numerically solving the governing equations using commercial CFD software FLUENT 6.3.26. The second order implicit time marching scheme was used to discretize the temporal derivatives. To simulate the experimental conditions reported by Shebeko *et al.* (1988), the computations were run for 60 s of flow time and 10^{-4} s time step, which was based on the time step independence study for each turbulence model. According to the conditions in the experiments of Shebeko *et al.* (1988), initially the quiescent air was filled in the cylinder at atmospheric pressure (101,325 Pa) and temperature 20 ^{0}C. Subsequently, hydrogen was released at velocity of 58.0 m/s for 60 s, and after the end of release of hydrogen, the hydrogen dispersion patterns were observed at various time steps. To simulate the conditions described above, flow is initialized from inlet of hydrogen and then air is patched at 20 ^{0}C and

1.01325 bar in the cylinder before starting computations. All equations, namely, continuity, momentum, energy and species transport (non-reacting species) were numerically solved using FLUENT 6.3.26. The second order upwind scheme was used for the discretization and the SIMPLE algorithm was used to treat the pressure-velocity coupling. For the code validation, hydrogen volume fractions are compared with computational results reported by Gallego *et al.* (2007) for the same geometry as that considered by Shebeko *et al.* (1988). The average deviation between the present computations and those by Gallego *et al.* (2007) was approximately 7.3% (Figure 4).

Figure 4: Comparison of Present Computations with Those Reported in the Literature



5. Results and Discussion

Figure 5 shows the volume occupied by the hydrogen at the end of 60 s after the release of hydrogen. Initially, hydrogen disperses due to the momentum in the discharge jet until it strikes the top of the vessel. Subsequently, the dispersion is mainly due to the buoyancy as once the jet strikes the top of vessel, it loses its momentum and therefore the subsequent flow is driven by the buoyancy only. Once hydrogen reaches the top of the cylinder, it starts flowing horizontally and starts occupying the space below. At the end of 60 s mixture above, the jet contains maximum hydrogen, but it is much leaner than the stoichiometric ratio and this indicates that

the accumulated mixture does not have large danger. Figure 6 shows dispersion patterns in the flammable zones after the flow of jet is cut off. It clearly shows the major flammable zones are at the top wall of the cylinder. It can be seen that the flammable hydrogen region is quite large, but gas is diluted which is expected to attain low

Figure 5: Volume Fraction of Hydrogen at the End of Release of Hydrogen (60 s)

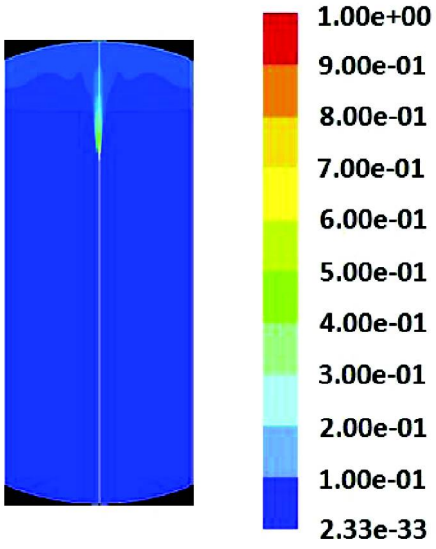
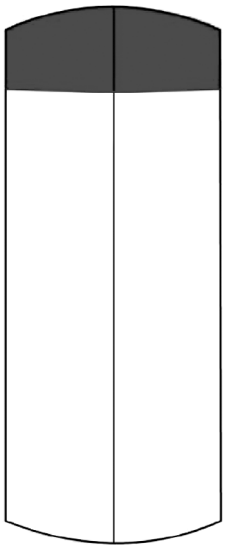


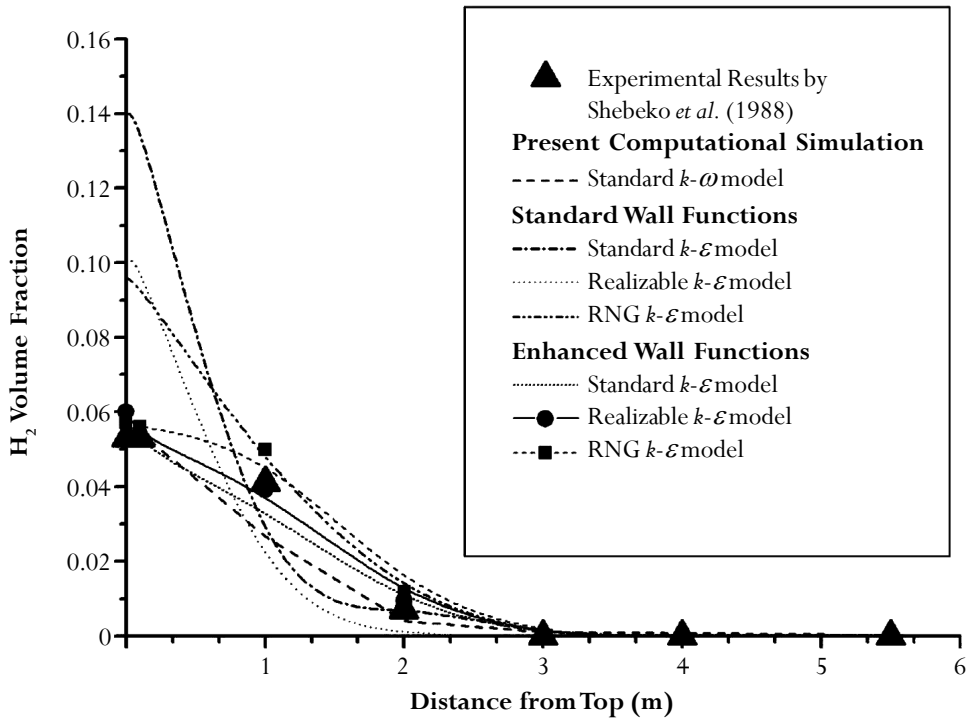
Figure 6: Flammable Zone of Hydrogen at 120 s After End of Release (Volume Fraction in Between 4% and 75%)



pressures when ignited as the mixture is quite lean. As the density of hydrogen is approximately 15 times smaller than the density of air due to the buoyancy, hydrogen always accumulates at the top of the container, and therefore the danger of fire at the ground level is small compared to the situation when other gaseous fuels, such as methane are used. Figure 5 shows a faster dispersion of hydrogen and therefore the danger of fire will be large, if a large volume of gas is leaked or if the size of leak is large.

Figure 7 shows the comparison between the present results and the experimental results of Shebeko *et al.* (1988) using different turbulence models and different wall functions. It is clear that there is a large deviation between the results predicted by different mathematical models. However, the predictions by realizable k-ε model using the enhanced wall functions are in good agreement with the experimental data of Shebeko *et al.* (1988). A small deviation between the two is probably due to the assumptions of axisymmetry and isotropy used in the turbulence models, but in reality the flow is highly anisotropic. There are two approaches to bridge the gap

Figure 7: Comparison of Computed Hydrogen Volume Fraction Near Centerline After 120 s of Flow Cut off with the Experimental Results of Shebeko *et al.* (1988)



between the viscous sublayer region near to wall and the fully turbulent region. One method is to perform computations right up to the wall using unstructured mesh that is very fine in the near wall region and rather coarse at other places and the second is the wall functions approach. The first method is computationally expensive due to the need for a fine mesh. However, the wall functions approach is reasonably accurate as well as computationally less expensive. The standard wall functions needs coarse mesh so that $y^+ = 30$ is at the first grid point, but enhanced wall functions require rather fine mesh in the viscous sublayer region. In general, the k-ω and k-ε models with enhanced wall treatment provide quite accurate results compared to those by using the standard wall functions.

Conclusion

- The high convective region associated with hydrogen jet causes its faster dispersion with air in the container.
- The impingement of the hydrogen jet on the top also leads to faster dispersion of hydrogen.
- There is a natural convection due to the nonuniform density difference in the vessel. Further, due to variable density and stratification a wave-like motion is detected in the vessel.
- The mass diffusion is turbulent and due to a high turbulence the rate of dispersion of hydrogen within the vessel is high.
- All versions of k-ε model with the standard wall functions fail to predict the dispersion behavior in case the leakage size is quite small compared to the size of the computational domain selected for investigations.
- All versions of k-ε models with the enhanced wall treatments and standard k-ω model predict results in good agreement with the corresponding experimental results.

References

1. Choudhury D (1993), "Introduction to the Renormalization Group Method and Turbulence Modeling", Fluent Inc. Technical Memorandum TM-107.
2. Dewan A (2011), *Tackling Turbulent Flows in Engineering*, Springer, Berlin, Germany.
3. FLUENT Inc. (2006), "Fluent 6.3 Documentation", available at http://www.fluent.com

4. Gallego E, Migoya E, Martín-Valdepeòas J M *et al.* (2007), "An Intercomparison Exercise on the Capabilities of CFD Model to Predict Distribution & Mixing of Hydrogen in Closed Vessel", *Int. J. Hydrogen Energy*, Vol. 32, pp. 2235-2245.

5. Launder B E and Spalding D B (1974), "The Numerical Computation of Turbulent Flows", *Computer Methods in Applied Mechanics and Engineering,* Vol. 3, pp. 269-289.

6. Olvera H A and Choudhuri A R (2006), "Numerical Simulation of Hydrogen Dispersion in Vicinity of a Cubicle Building in Stable Stratified Atmosphere", *Int. J. Hydrogen Energy,* Vol. 31, pp. 2356-2369.

7. ShebekoY N, KellerV D,Yeremenko OY, Smolin I M, Serkin M A and Korolchenko A Y (1988), "Regularities of Formation and Combustion of Local Hydrogen–Air Mixtures in a Large Volume", *Chem. Ind.*, pp. 21-24.

8. Shih T-H, Liou W W, Shabbir A, Yang Z and Zhu J (1995), "A New k-ε Eddy-Viscosity Model for High Reynolds Number Turbulent Flows-Model Development and Validation", *Computers and Fluids,* Vol. 24, pp. 227-238.

9. Swain M R, Filoso P, Grilliot E S and Swain M N (2003), "Hydrogen Leakage into Simple Geometry Enclosures", *Int. J. Hydrogen Energy*, Vol. 28, pp. 229-248.

10. Venetsanos A G, Huld T, Adams P J and Bartizs G (2003), "Dispersion and Combustion Modeling of Accidental Release of Hydrogen in as Urban Environment", *J. Hazardous Materials,* Vol. 105, pp. 1-25.

11. Versteeg H K and Malalasekera W (2007), *An Introduction to Computational Fluid Dynamics*, Pearson Education Limited, 2nd Edition.

12. Vudumu S K and Koylu U O (2009), "Detailed Simulation of Transient Hydrogen Mixing, Leakage and Flammability in Air in Simple Geometries", *Int. J. Hydrogen Energy,* Vol. 34, pp. 2824-2833.

13. Wilcox DC (1998), "*Turbulence Modeling for CFD",* DCW Industries Inc., La Canada, California.

14. Wilkening H and Baraldi D (2007), "CFD Modeling of Accidental Hydrogen Release from Pipelines", *Int. J. Hydrogen Energy,* Vol. 32, pp. 2206-2215.

Appendix

Nomenclature

U	Mean velocity
E	Total energy
k	Turbulence kinetic energy
h	Enthalpy
Sc	Schmidt number
D	Diffusion coefficient
L	Height of cylinder
D_c	Diameter of cylinder
d	Leak diameter
T	Temperature
k	Thermal conductivity
t	Time
Pr	Prandtl number
J	Diffusion flux

Subscripts

i,j,k	Index notations
t	Turbulence parameters

Greek Symbols

ρ	Density
μ	Dynamic viscosity
ν	Kinematic viscosity
ε	Dissipation rate
ω	Specific dissipation rate

Reference # 60J-2012-05-03-01